Studies of Low Energy Gammas and Event Backgrounds in Milagro

Magdalena Gonzalez, Jim Linnemann, David Noyes

July 31, 2003

1 Summary

We have looked at gross characteristics of low energy Monte Carlo gammas compared with data, in order to decide where to improve selection of low energy gammas. We concentrate on low energy Monte Carlo gammas passing the lowest-threshold trigger. We have also looked at pulser data as a sample of the background. Our conclusions are:

- The gamma enhancement variable X_2 has poor efficiency at low energies. We will concentrate on trying to find an improved variable suitable for low energy gammas.
- X_2 may also have problems at higher energies for events with many air shower tubes hit.
- Noise may be affecting the efficiency of lowest-threshold trigger, but for now we will concentrate on the data taken with the present trigger.
- The angle fitter efficiency is poor if good angular resolution is required. However, this is caused more by lack of good hits, than by noise.
- We will not for now concentrate on improving reconstruction, assuming that useful physics can still be done with 5 degree resolution.
- Cosmic rays hitting the pond from events uncorrelated with a triggering shower are part of up to 30% of all events.
- This background may interfere with hadron-layer quantities, particular for low-multiplicity events.
- This background may make reconstruction of low energy showers difficult, but the loss of efficiency should be small because few tubes are hit in the air shower layer in such events. Thus, we are not presently pursuing their removal from the fitter.
- There are a number of unsatisfactory features in the default noise model in the Monte Carlo. However, we are not presently pursuing improvements. Such improvements will be needed to quantify the efficiency loss from cosmic ray backgrounds interfering with hadron separation variables using the muon layer heavily. Improvements would also be needed to understand the importance of changing the lowest-threshold trigger. It might also become important in the quantitative cross-checking of the Monte Carlo for hadrons with the data, or possibly to study improvements in the angle fitter.

2 Introduction

The goal of this part of our study was to characterize the problems specific to low energy gamma rays, with a view to effectively using them for gamma ray burst searches. We decided to concentrate on 1) gammas with $100 \leq E_\gamma \leq 300$ GeV, based on expected cosmic absorption (as suggested by Brenda

Dingus) and 2) gammas passing only the 20-tube trigger, since this was the new chunk of data acquired for this purpose. We hope anything we learn would also help other gammas. After characterizing the problems with this data, our intention is to try to improve selection of gammas for these events by addressing these problems in order of their importance.

Our full MC gamma sample includes energies from .1 to 100 TeV, generated with a spectrum proportional to $E_\gamma^{-2.4}$, with a preselection requirement of 10 hit tubes in the event. A reasonable number of dead tubes was included in the simulation, though there was no attempt to force exact matching with the data sample with which we compare from time to time. The gamma MC sample was generated with a distribution in core radius with respect to the center of the pond proportional to r_c, though the physical distribution of core distances would be instead proportional to r_c^2. Most events at large core radius do not trigger, so this technique concentrates most of the CPU time on events which have better odds of triggering. However, to compensate for the non-physical distribution, the events must be plotted with an event weight of r_c.

In what follows, we will use T20 (or, in graphs, trigtype == 4) to refer to the 20-tube trigger with the 75% rise time (1/8 to 7/8) cut of 50 ns. There is also T50, which requires 53 tubes and includes a 75% rise time cut of 87.5 ns, and T75, which requires 74 tubes, with no rise time requirement, and T20 without the rise time requirement, but prescaled by a thousand. Further, the T20 tube threshold is often raised to limit the experiment dead time; it currently has a 25 tube threshold.

3 What We Think We Know Now

3.1 X_2

Scanning data and low-energy simulated gammas gives the impression that these events are not easy to tell apart. Currently, the only variable we have to enhance gammas with respect to hadronic cosmic rays is $X_2 = N_2^\mu / PE_{max}^\mu$, the ratio of the number of muon layer tubes with 2 or more PE's (equivalent photo electron pulse height), divided by the largest pulse height measured in any muon layer tube. One concern with this variable is that its behavior as a function of shower energy is far from obvious. The standard cut for this variable is $X_2 > 2.5$, which was used for the Crab analysis, and optimized for data taken with T50 and T75, for which gamma showers typically have higher energies than for T20.

The efficiency of $X_2 > 2.5$ is significantly lower for T20. Figure 1 (left panel) shows efficiency[1] as a function of $Log_{10} E_\gamma$ for gamma MC events passing any trigger, and for those also passing the $X_2 > 2.5$ cut. On the x axis scale, 3 is 1 TeV. The efficiency above 10 TeV is above 50%, but drops to near 10% at low E_γ. The right panel shows that for T20, the situation is even worse, with the X_2 efficiency about 11%, for most energies, for events which satisfy only the T20 trigger. Other checks show an X_2 cut efficiency of 31% for all triggers combined, and 53% for the triggers other than T20. **The X_2 cut efficiency varies strongly with energy and air shower tube multiplicity (and thus by trigger type).**

To understand this better, in Figure 2 we show (for data on the left, and MC gammas on the right) the mean value of X_2 as a function of the number of air shower layer tubes hit. The X_2 distribution for MC gammas is not affected by standard MC noise (described below). The T20 trigger covers the left part of these plots, roughly from 20 to 50 tubes (the x axis is the number of calibrated tubes, which is close to, but not the same as, the analog sum used by the trigger). As expected, X_2 is generally lower for data than for gammas. A striking feature of the plots is the strong dependence of X_2 with the number of air shower tubes hit, despite the fact that X_2 involves only variables measured in the muon layer.

For both data and gamma MC, there is a linear rise in mean X_2 with the number of air shower

[1] The error bars in these and the following plots of means, or efficiencies, as a function of another variable, represent the determination of the mean (in this case of the efficiency), rather than the rms spread of that value in the data, so that heavily populated bins can have small error bars even when the data are quite variable.

tubes hit between 20 and 50. In the data, the initial rise is sharper, and X_2 is roughly independent of the number of air shower tubes from 60 to 250 tubes, when, perhaps surprisingly, X_2 begins to drop. For gammas, mean X_2 continues to rise beyond the 50 tubes, reaching a maximum around 200 tubes and staying more or less constant until 350 tubes, when mean X_2 rapidly decreases with the number of hit tubes. Also visible are some irregularities near trigger thresholds. Clearly, gammas showers striking small numbers of air shower tubes are inefficient with our X_2 cut, but surprisingly, so apparently are gammas with high numbers of tubes. To the extent that energy and the number of hit air shower layer tubes are correlated, it would appear that **gamma efficiency is limited by our X_2 cut at high energies**. It is true that the T20 trigger also suppresses X_2 for data. However, an X_2 cut of 2.5 still has an efficiency of 4% for data, giving an estimated Q factor of 0.5 for MC gammas compared to data, where the Q gives the factor by which the (Gaussian-limit) statistical significance would increase by applying a cut. A useful expression for Q is $Q = \epsilon_\gamma/\sqrt{\epsilon_d}$ where ϵ is the cut efficiency. This assumes that most of the data are hadrons, so that Q_d is appropriate. That is, applying **the standard X_2 cut for T20 data lowers instead of raises the statistical significance. The X_2 cut value is too high for T20 gammas, and the efficiency poor.**

The strong dependence of the X_2 distribution on the number of hit air shower tubes suggests making the cut a function of this variable.

Because the X_2 efficiency is so low for T20, there is not much difference between scanning all our sample, or only those which failed X_2.

The left panel of figure 3 exhibits the expected correlation of gamma energy with the number of air shower tubes hit. The right panel shows a decrease of the average shower radius with the number of hit tubes, demonstrating the tendency of showers hitting more air shower tubes to have struck the pond directly. Interestingly, **in the T20 region, there is a fairly strong negative correlation between tubes hit and radius, probably induced by the tight rise time cut**.

3.2 Triggering Problems

The trigger efficiency differs notably with noise on vs noise off, as shown in Figures 4-5, which plot various trigger efficiencies with and without noise for MC gammas. Table 1 shows this quantitatively.

		<300GeV	>300 GeV
any trigger	no noise	3294	15971
	noise	2341 (-29%)	13182 (-17%)
excluding T20	no noise	902	9491
	noise	999 (+11%)	9973 (+5%)
T20 only	no noise	2392	6480
	noise	1342 (-44%)	3209 (-51%)

Table 1: MC Gamma Events Passing Various Triggers, and Effects of standard MC Noise

From the table we see that over 70% of the low energy gammas and 40% of triggered higher energy gammas up to 100 TeV depend on the T20 trigger. The noise lowers triggering efficiency for low energy gammas by 29%, but lowers high energy gammas trigger efficiency by only by 17%. For T20, the noise losses are 50%. For the higher-multiplicity triggers, noise instead increases the triggering rate by 5-10%.

We notice that turning MC noise on has opposite effects on T20 and the T50 triggers. This is because noise hits widen the rise time. Figure 6 shows the effect with the current trigger simulation and noise model. In the left panel, strikingly, **the T20 cut is in middle of the rise time peak even without noise, implying the MC estimate of the T20 efficiency has large systematic**

errors; perhaps it can be more reliably estimated with the prescaled 20 tube trigger with no risetime cut. Two other effects are apparent. First, the rise time peak appears to be broadened, and shifted upwards by noise, causing a significant number of events to fail the 50ns cut (the number in the broadened peak is comparable to the original peak). Second, with noise, a second peak appears at 130 ns instead of 40ns (with about 2/3 as many events as the original peak). **The cause of this secondary peak should be investigated.** It is not clear whether the second peak mostly includes events from the original peak, or low-multiplicity events now passing the 20 tube cut. It is also unclear whether this is only a software effect, or reflects actual trigger behavior[2]. Similar effects are visible when the gamma energy is restricted to less than 300 GeV (right panel), though the noise-free rise time distribution is slightly wider at low energies. The net result, according to the simulation, negatively impacts T20, which has a tight rise time cut; further, since there are few tubes, noise hits have a larger fractional effect. This effect overcomes the expected increase in the number of events passing the 20-tube cut by having extra noise hits allow events with fewer than 20 tubes to trigger. The rise time effects are weaker for T50, and noise does increases the T50 rate.

3.3 Angular Reconstruction Problems

In Figure 7 (left panel), we plot the relative number of reconstructed noise-free MC gammas passing T20. The efficiency for reconstructing within 1.5° of the MC position is only 20-30%, though if this criterion is loosened to 4.5°, the efficiency rises to 70-80%. The right part of Figure 7 shows the same thing, but with the Monte Carlo noise turned on. In this case, we see that the efficiency changes somewhat, but not drastically, for a given required reconstruction accuracy. **The reconstruction problems are intrinsic to having few tubes to work with, rather than being dominated by noise.**

For now, we won't chase ideas about identifying noisy tubes and trying to remove them from the fit. David Noyes has tried many potential improvements to the fitter and will summarize this work elsewhere.

3.3.1 Overlap Among Problem Events

We studied whether the events failing X_2 are the same events which also have weak angle reconstruction. Unfortunately, they are not: poor fits do not stand out as low values of X_2. However, since X_2 and the reconstruction accuracy do are weakly correlated, they can be dealt with independently. This can be seen from Figure 8, which shows, from top to bottom, the X_2 distribution for all reconstructed events, for those reconstructing from $1.5 - 4.5°$ of the MC direction, and for those reconstructing within 1.5° of the MC direction. There is a rather mild dependence, with the mean X_2 increasing from 1.31 for all reconstructed events to 1.49 for those within 1.5° of the MC direction.

4 Characterization of Noise

We took data with a pulser trigger, uncorrelated with any other trigger. This should give an accurate picture of the actual "noise", or "background event", which nature overlays on our actual triggered events (at least within the approximation that the "noise" does not affect triggering). We were particularly interested in the noise for T20 events, where the number of noise hits is larger relative to the triggered hits than in other triggers. We believe we can learn much of what we need to know about noise by looking at it, before incorporating it in the Monte Carlo.

[2]Erik Blaufuss notes that the algorithm works in 12.5 ns bins, and looks back 125ns (10 bins) and forwards 187.5ns (15 bins); perhaps the 130ns peak is related to hits coming in the earliest look-back bin for events which otherwise would not pass the multiplicity cut. David Noyes notes that the secondary peak goes away when the threshold is raised to 30 tubes.

4.1 Clustered Noise Events

Scanning the pulser data in the event display, it is obvious that a bit less than a third of the events contain neighboring tubes hit in both the air shower and muon layers. Our criterion for a non-random cluster was fairly loose: we wanted to see at least one calibrated hit in the air shower layer in reasonable physical proximity (a few tubes) to at least one hit in the muon layer. The criterion is loose because the incidence angle is unknown. Many events did not resemble random hits uncorrelated between layers, but have correlations, presumably induced by physics. As will be seen later, both hits must fall within a $\pm$200ns window about the (random) trigger time to be seen in the event display. A "typical" event can be seen in Figure 9.

A slightly more quantitative assessment can be made by considering only events with 7 or more calibrated hits in the muon layer; these events (by a hand scan with the "criteria" above) have an association between the muon hits and an air shower hit 2/3 of the time, so are a decent proxy for having found a "muon" by eye. The fraction of pulser events which pass this cut of CALhitmu>6 is 30%. The number of muon tubes with substantial pulse height is demonstrated in Figure 10 (left panel), which shows the number of tubes with 2 PE's or more (for clarity the bins with 0 or 1 have been suppressed). The 2PE threshold is relevant for the calculation of the hadron rejection variable X_2. It is readily seen that there are typically 10 tubes in events which do have a cluster. The selection criterion above has no effect on the size or location of peak, so it is a property of the data, not the selection criteria. The cut does enhance the fraction of events in the peak, as claimed.

The muon finder identifies only 5.6% of events as having muons; more than 99% of the muons found pass the CALhitmu $>$ 6 cut. One might question the efficiency of the muon finder (perhaps 20% of my candidate "associations"), but its purity certainly seems good; conversely, the CALhitmu cut might be overly loose, but its efficiency for muons seems to be good. The angle fitter is not very interested in these pulser events: only .7% pass the fitter, with an average of 10 or so tubes in the fit.

Figure 10 (right panel) shows the distribution of pulse height for muon layer tubes with and without the CALhitmu$>$ 6 cut. Even with the very low threshold, about 80% of all muon hit tubes are associated with this class of events, larger than the 69% expected (with mean number of hits of 6.9 and an independent Poisson is assumed); the association with clusters is more striking for tubes above 2 PEs than for the calibration threshold, which is about .1 PE (The discussion of figure 12 below gives a bit more information about events with muon tubes with more than 2PE's). You will also notice in the pulse height distribution a small peak at roughly 10 PE's. Similar plots for the air shower layer show 60% of the hits are associated with clusters, about twice the random 30% level, while only 32% of outrigger events come on the muon clustered events.

	All Pulser Events			Events with CALnhitmu>6			
Layer	Calibrated	>2PE	>8PE	Calibrated	>2PE	>8PE	Singles kHz
AS	3.9	0.9	0.4	8.1	4.3	0.9	24
Mu	7.2	2.3	0.8	19.4	7.1	2.6	68
Outrigger	2.0	0.9	0.3	2.1	1.0	0.4	30

Table 2: Mean hits per event for various layers, and implied singles rates (from number of live tubes, and Calibrated tubes/event), assuming 400 ns sensitive time.

Table 2 above summarizes the number of hits per event seen in the pulser data, and, the resulting estimate of the singles rate per tube, which is consistent with the observed range. One can also estimate the tube occupancy due to electronic noise only by from the mean for the 30% of events with more than 6 muon layer hits by $\mu_N = (\mu - .3\mu_6)/(1 - .3)$. Roughly 2 hits per event for each layer are expected from electronic noise alone; these hits would be expected to be isolated within their layer and uncorrelated with other layers; the rest of the hits would be from events with inter-layer correlations. The inferred noise hits per event corresponds to a rate $\mu/400ns$, or 12, 18, and 28 kHz for typical tubes in the three layers, or respectively 50, 26, and 93% of the singles rates.

Figure 11 shows that the number of tubes hit in the air shower layer is typically one for a moderate pulse height cut of 2 PE's, markedly less than the number of hits in the muon layer. This is consistent with single-particle cosmic rays dominating the origin of the clustered events. This also is fortunate, as this would suggest that the background events will not seriously perturb the angle fitter, so long as we continue to base the angle fit on the air shower layer and require 2 PE's for the first fitting iteration.

For completeness, we also studied the distribution of X_2 in the pulser data. The results are shown in Figure 12. Events where no X_2 was found, because there were no muon tubes with 2 PE's or more, are excluded from this plot. The left panel shows that the distribution is largely below $X_2 = 0.5$, not surprising since the threshold for registering an X_2 value is one tube with $\geq$ 2PE's, giving $X_2 = 1/2$. A slightly higher pulse height would force a single-tube event to lower X_2. The correlated muon events have X_2 a bit higher than the average, as can be seen in the right panel of figure 12. Here the events with 7 or more calibrated muon tubes are contrasted with from all events with one 2PE tube; these 7 tube events, shown in red, form the bulk of all events 2PE events.

We looked at the pulse height of the maximum muon tube. Figure 13 shows the spectrum for all pulser events. The spectrum drops steeply, but there is a local maximum near 30PE's (presumably related to muons) and a much smaller one near 5000PE's, representing saturated tubes. **Surprisingly, the pemax spectrum continues out to 25000. This should be investigated, as PEmax is sensitive to single mis-calibrated tubes**.

4.2 Timing Anomalies

If these pulser triggers are indeed due to randomly-arriving cosmic ray events, then the time distribution should be flat within the cuts imposed by the software. Figure 14 (left panel) shows the time distribution for hit muon tubes in the pulser events, which has an unexpected enhancement at early times. Erik Blaufuss and David Williams agree that this is caused by early hits whose first two edges fall outside the time window, but whose third and fourth edges fall within the window. The edge finder apparently assigns them a low pulse height around the time of the third and fourth edges. As predicted, we found an excess of early times at small pulse heights. Further, the right panel of Figure 14 verifies that the behavior changes when the time window is widened from 400 to 600 ns, confirming that **the non-flat time distribution in pulser data is a feature of the software**, rather than a feature of the pulser data (and physical background "noise" in real events). **One might argue that the edge finder ought not to do this**, but in any case, it's another small wrinkle in the actual behavior of noise which the Monte Carlo won't model correctly, since neither MC data nor MC noise pass through the edge finder.

4.3 Comparison of Observed Rates with Expectations from Cosmic Rays

These visually-clustered events are mostly cosmic ray muons, as can be seen by the rough estimate of the expected rate which follows. Out of time hits are excluded (not "calibrated") in the edge finder by a cut at $\pm$200ns, or a 400 ns sensitive window. This cut on hit times therefore applies to the core fitter, X_2, the angle fitter, and the event display.

With $.4\mu s$ sensitive time, a 30% fraction of clustered events implies a rate of $.30/.4\mu s = .75MHz$ of muons to the pond. At Milagro's altitude, according to Gaisser's review in the Review of Particle Properties, the vertical rate of muons > 1 GeV is perhaps $100/m^2/sr/s$. The pond area for such coincidences is somewhere between $1500 - 4800m^2$ (area of the air shower and muon layers), depending on the angular acceptance of muons for this loosely defined coincidence, and the 41° Cherenkov angle). Gaurang Yodh estimates our angular acceptance as about 1.5 steradians (for a $cos^2\theta$ angular distribution); Gaisser's review equates a vertical muon rate at sea level of $70/m^2/sr/s$ with a horizontal detector rate of $1/(cm)^2/min = 167/m^2/sr/s$, which would imply 2.4 sr. In addition, we are sensitive to muons below 1 GeV if the overlap criterion is one tube in the air shower layer and several in the muon layer; Gaurang suggests this could raise this effective rate by up to a factor of two. This leads to an estimated rate of

$$100/m^2/sr/s \times 2 \times 2sr \times (1500 - 4800)m^2 = (.6 - 1.9)MHz$$

Treating the Poisson statistics a little more carefully, we could set the observed fraction of moun events to $p = .3 = P(>0) = 1 - P(0) = 1 - e^{-\mu}$; this yields $\mu = -ln(1-p) = .36$, and $R_\mu = \mu/T = .36/.4\mu s = .9MHz$. Poisson statistics implies perhaps 10% of muon events have multiple muons, consistent with a visual scan. An effective muon rate of .9 MHz the pond is within the estimated range, (particularly since there are further small contributions from electrons and hadrons), so there is no obvious need for other sources (electronic pickup, or flashing tubes) of correlated hits beyond single-particle cosmic rays, which we now simply call "muons". As a rough cross-check, if some 5 muon layer tubes are hit for each cosmic ray, that yields a muon layer rate of 5MHz, compared to an observed rates of 1 (9) MHz from the scalers for high (low) threshold muon rates, suggesting that a significant fraction of the muon tube rates are due to cosmic rays; this is consistent with the observed 80% of muon hits coming from high-multiplicity events.

5 MC Noise Problems

The standard noise model in the MC could enhanced in several ways.

5.1 Independent Hits

The current noise model inserts hits based on tube singles rates, with no correlation among tubes. However, it's clear that a good fraction of the singles rate actually comes in the forms of correlated muon hits. **While code exists to use pulser data for noise, it is not in the standard library**.

5.2 PE distribution of noise

The default MC noise hits all have exactly 1.00 PE's (conveniently too low to bother X_2 or the angle fitter first pass). While most hits in the pulser data are near 1PE, a significant tail extends beyond that level (see Figure 10). **The noise we are fighting is different than what we've been simulating**. Compared to the present MC noise, most events will be cleaner, but those with a muon will be dirtier. Those effects go in opposite directions, so we'll have run the Monte Carlo with a different PE distribution to see what its actual effects are.

5.3 Excessive Politeness

If there is a MC hit for the tube, the current code just ignores the potential noise hit. This is way too polite, and suggests the Monte Carlo may overestimate efficiency.

5.4 Doesn't Model Electronics or Edge Finder

The Monte Carlo doesn't produce raw data, or even edges. While that's not strictly necessary, probably a simple simulation of the electronics is needed to avoid having to choose between the noise or MC hit. We might have early noise change both the event time and PEs, and late noise change only the PEs.

5.5 How Important is it to improve the MC noise model?

Milagro already has code for incorporating the pulser data into the Monte Carlo. Using this code instead of the default noise code would cure the independence, and PE distribution problems, but the code still would have to be improved to address the modeling and politeness problems.

We decided this is not our highest priority now. Though the trigger may need improvement, we want to use the data we already have.

Muon clumps are a concern for hadron rejection, but even a 30% efficiency loss (essentially all events with muons) is not as severe as the losses from the current X_2 cut, which is more than a factor of 4 less efficient than the cut for higher energy gammas.

6 Conclusions

6.1 Issues we aren't pursuing, but should be taken up

- Re-evaluate effects of noise on X_2, triggering, and angular resolution with the present code, but using the pulser data.
- Fix the politeness and modeling problems in the noise model.
- Check the simulation of rise time in the MC; why does it give a double hump when noise is turned on?
- Improve the T20 trigger on the trigger card if the rise time losses are real. Gus Sinnis suggested counting multiplicity in a fixed time window; Brenda Dingus suggested calculating a 50% rise time instead of 75%. However, it might make sense to improve the noise model before deciding whether to pursue this.
- Improve the angular fitting for low multiplicity (if possible). To the extent that eliminating noise hits is important, perhaps one could look at isolation measures to remove uncorrelated noise hits. One could look at fitting only the bottom layer, but this might make muon backgrounds worse. Gus and David have suggested iterating the fits for the T20 trigger by successively dropping different candidate hits.
- The X_2 cut efficiency is energy and air shower multiplicity dependent. This must be accounted for, or perhaps better, optimized by making the cut a function of the air shower multiplicity. In the best of worlds, a better variable would be found.
- The X_2 cut efficiency may be altered significantly by the muon background, even for higher-multiplicity triggers; this is not currently accounted for.

We are not currently planning to pursue these ideas, since we are concentrating on the data at hand, but hope the Maryland group will check whether the trigger can be improved.

6.2 Acknowledgments

Thanks to Tony Shoup for help with the event display, and to Gaurang, Gus and Brenda for advice along the way. And, from Jim, thanks to Gus and Jordan for support which made it possible for me to spend a very enjoyable sabbatical, on which I learned many things. And thanks to my many Milagro collaborators who took the time to explain things to me, often more than once!

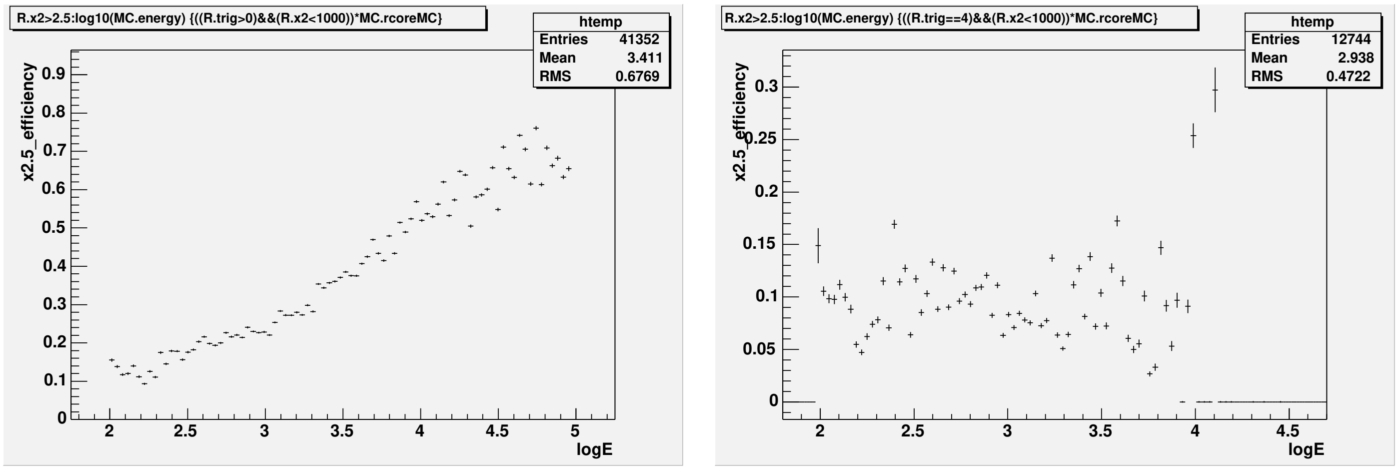

Figure 1: $X_2 > 2.5$ Efficiency. The fraction of MC Gammas passing the cut as a function of Log10 E(GeV). Left: For all events passing triggers. Right: For those events passing only the T20 trigger.

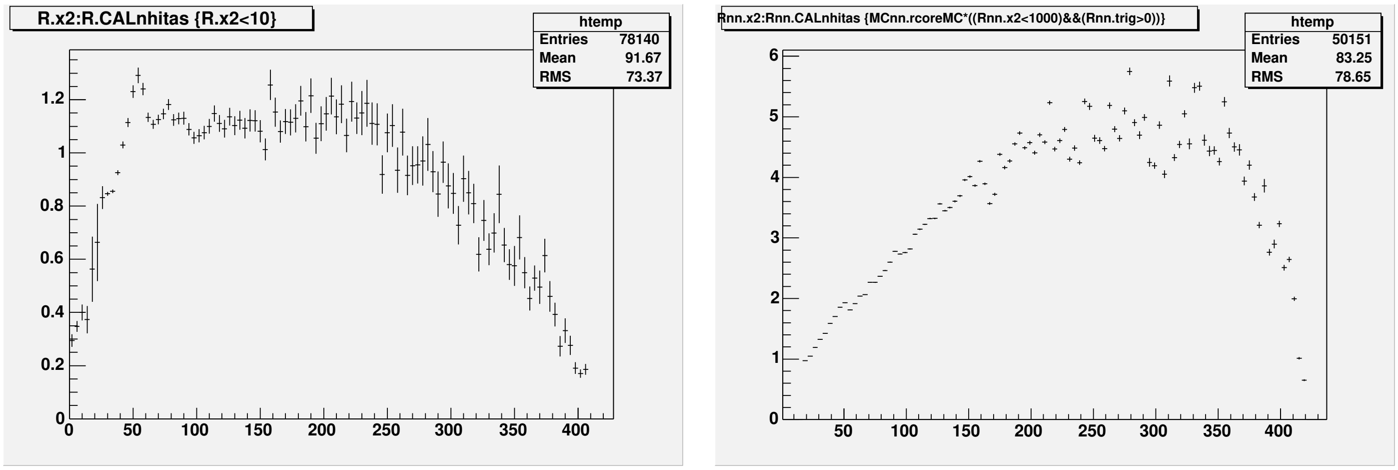

Figure 2: Mean X_2 as a function of the number of air shower tubes. T20 covers the region below 50 tubes. Left: For data events. Right: For gamma MC events.

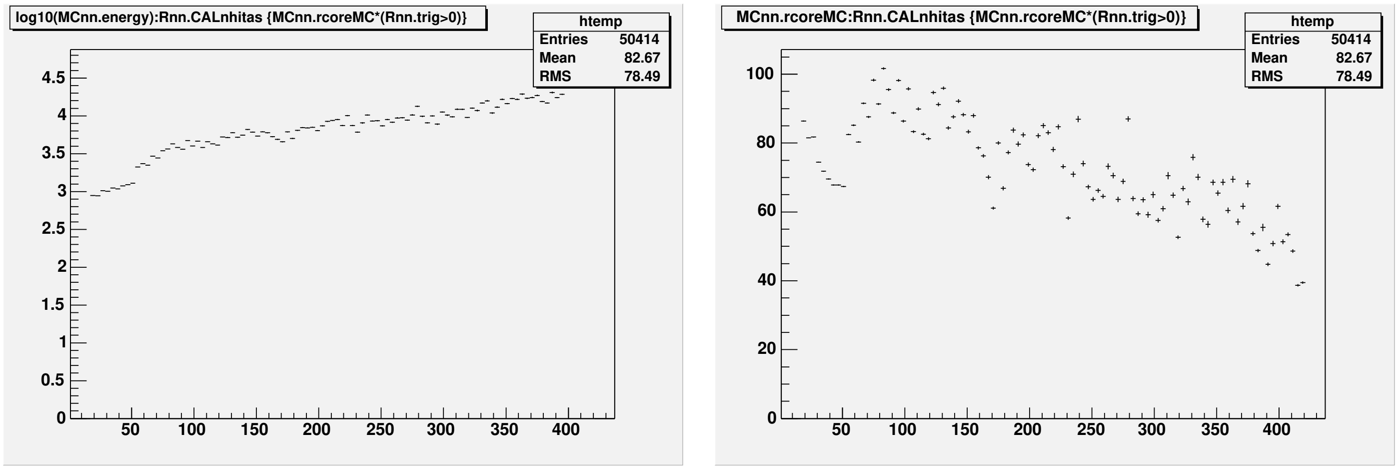

Figure 3: Left panel: mean [log10 E(GeV)] of MC gamma events as a function of the number of struck air shower tubes. Right panel: mean distance of shower from the center of the pond of MC gamma events as a function of the number of struck air shower tubes.

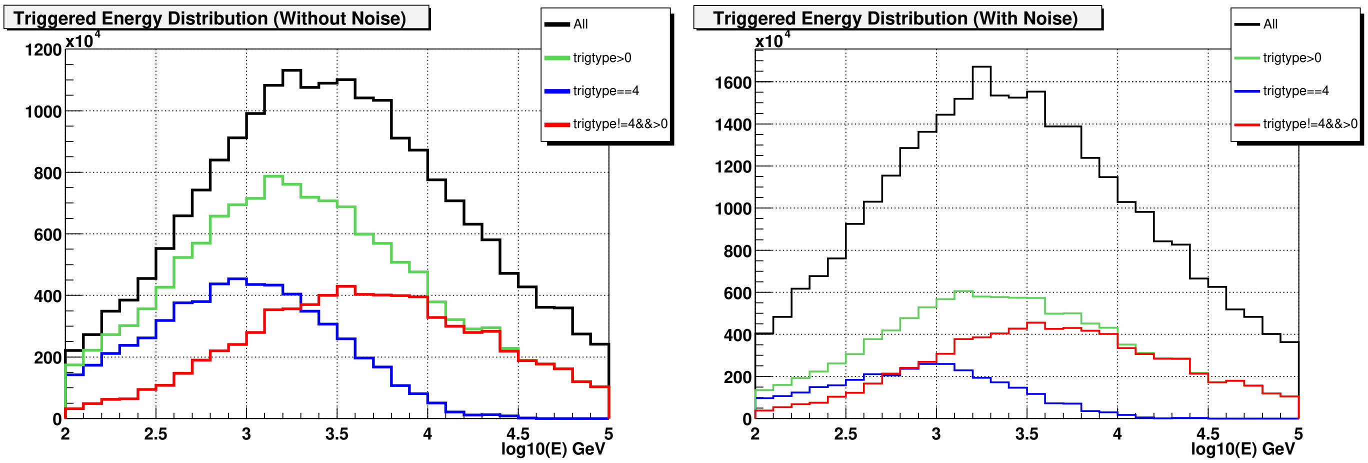

Figure 4: Triggered MC gamma energy distribution with and without standard MC noise Noise. “All” events fired 20 air shower tubes or more; trigtype ¿ 0 events pass some trigger, trigtype == 4 pass T20, and the others pass T50 or T75.

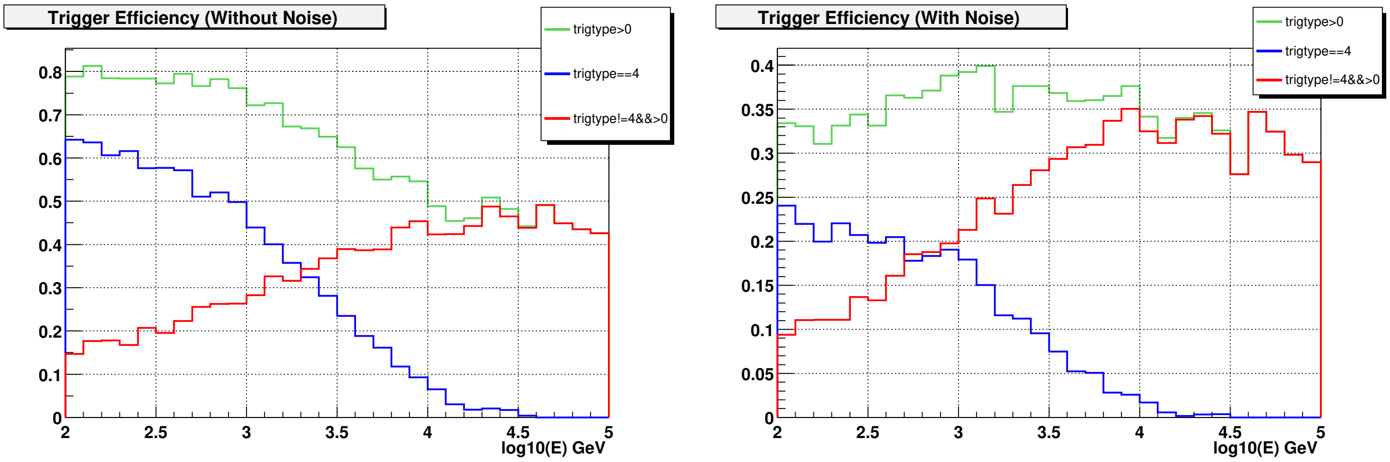

Figure 5: Trigger efficiency vs. energy for MC gammas without and with standard MC noise.

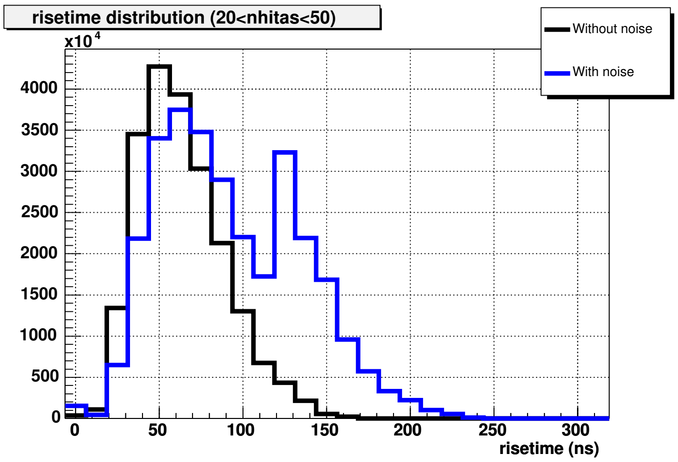

Figure 6: Left: Rise time with and without standard MC noise for MC gamma events with any energy, and 20 to 50 air shower tubes hit. These would be candidates only for the T20 trigger. Right: The same for gamma events with less than 300 GeV.

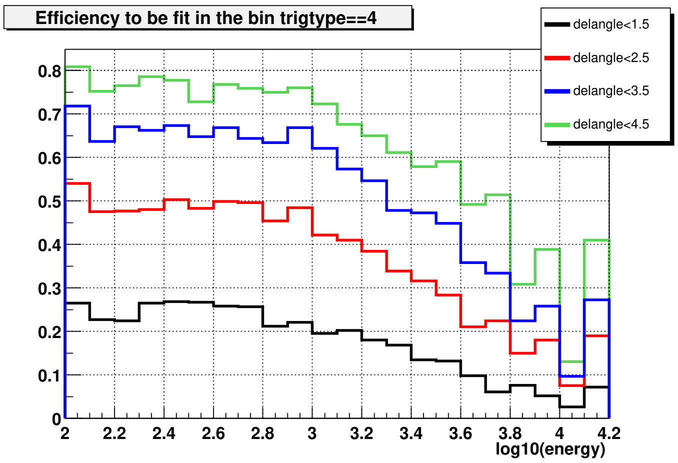

Figure 7: MC Gamma fit efficiency vs. energy without and with standard MC noise

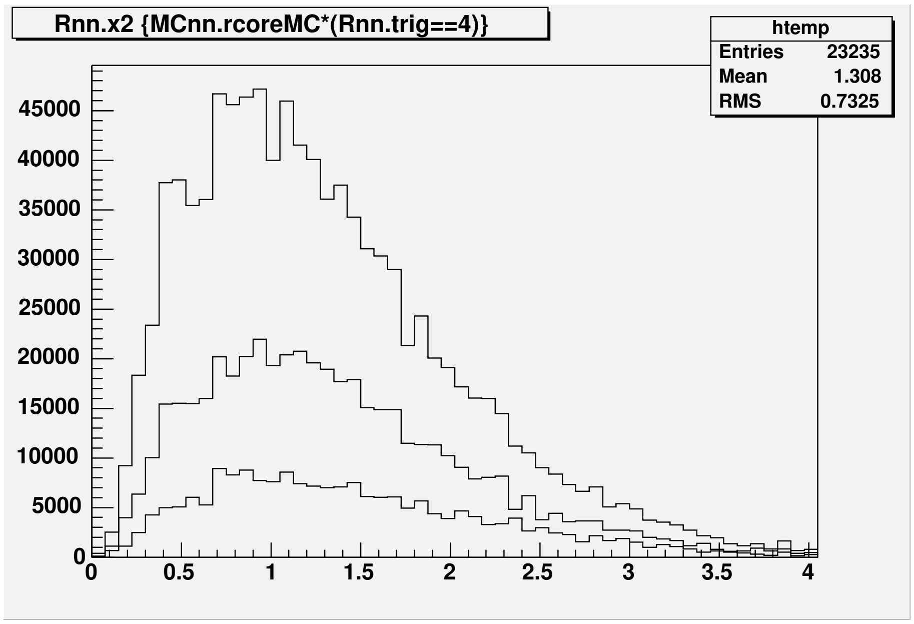

Figure 8: The X_2 distribution of MC gamma events passing T20, for various reconstruction quality requirements. Top curve: all events passing reconstruction. Middle curve: reconstructed angle between 1.5 and 4.5 degrees of MC angle. Lower curve: reconstructed angle less than 1.5 degrees from MC angle.

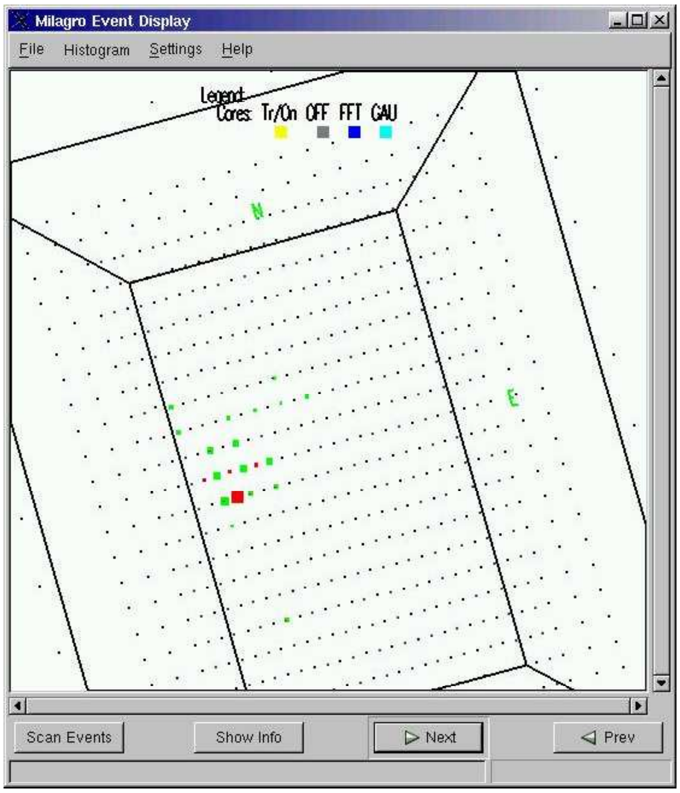

Figure 9: A clustered event from the pulser data with hits in both layers

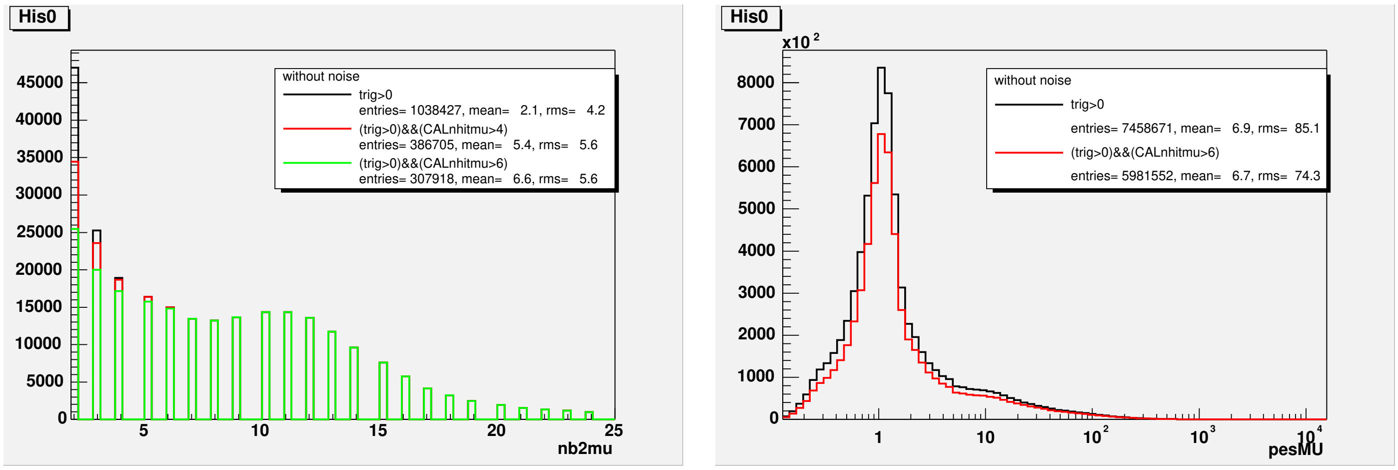

Figure 10: Left: Distribution of number of muon tubes with 2 or more PE's. Events with 0 or 1 tubes have been suppressed. Right: Distribution of PE's for muon tubes in pulser events.

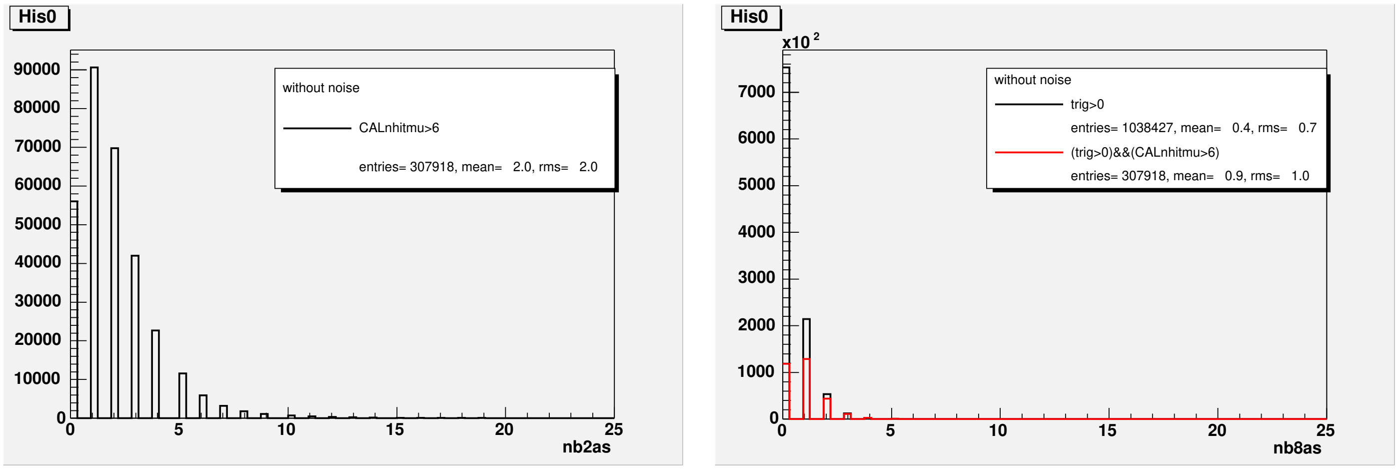

Figure 11: Left: Distribution of number of air shower tubes with 2 or more PE's when CALhitmu > 6 . Right: Same for tubes with 8 or more PE's

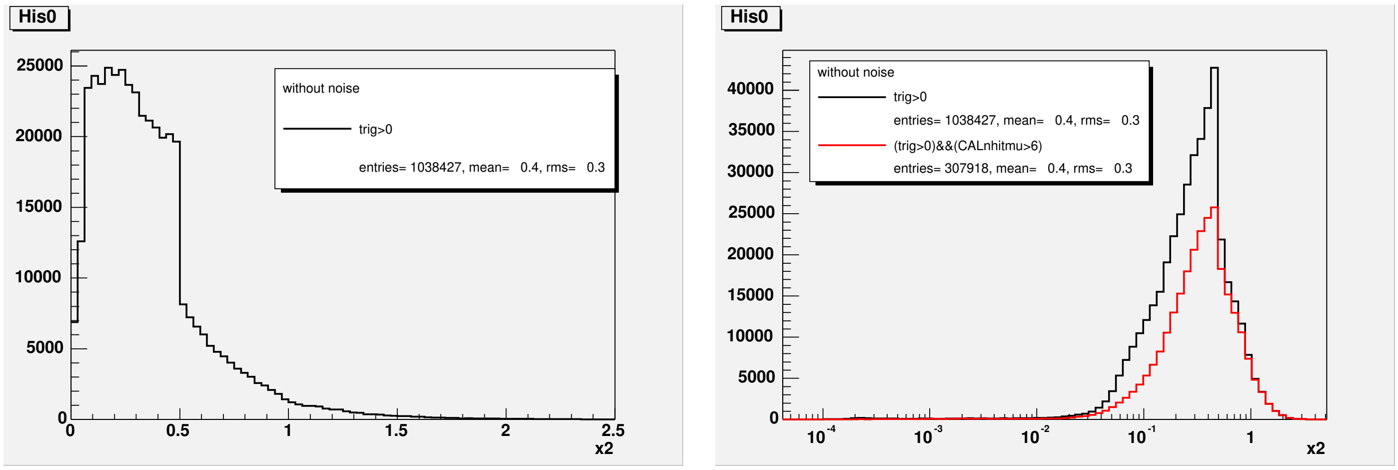

Figure 12: Left: X_2 distribution for pulser events with one or more 2PE muon tubes. Right: The same events, and, in red, the subset with 6 or more calibrated tubes. The calibration requirement requires much than 2PE's.

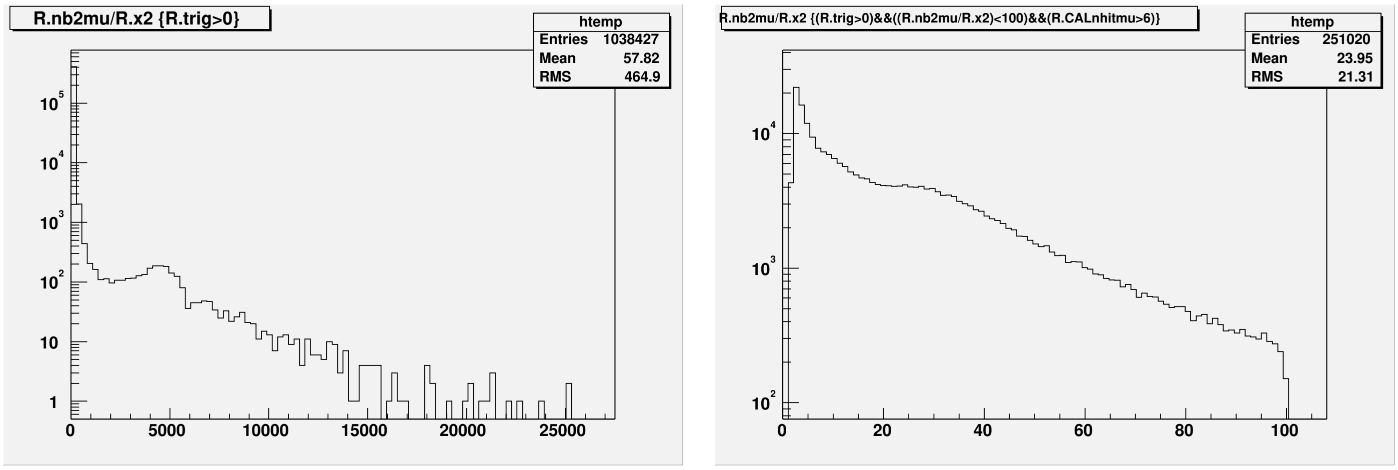

Figure 13: Left: Distribution of the muon tube with the largest number of PE's for pulser events with one or more 2PE muon tubes. Right: The same, but with the spectrum truncated at 100 PE's.

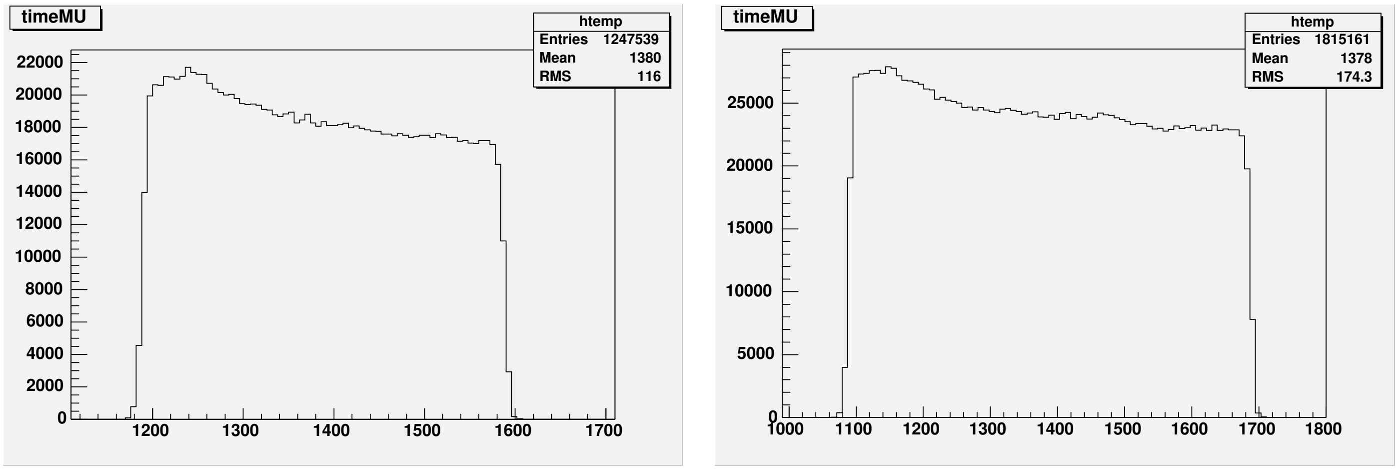

Figure 14: Left: Time Distribution for Muon Tubes in Pulser Data. The timing windows is the default 400 ns. Surprisingly, the distribution is not flat. Right: The same, with the timing window increased to 600 ns. The peak moves to the new edge location.